RESEARCH ARTICLE

ScienceAsia 29 (2003): **163-174**

Evaluation of the Compressible q-ζ Turbulence Model with Pressure Dilatation Term

Varangrat Juntasaro* and Arth Kanjanawongsamas

Computational Mechanics Laboratory (CML), Department of Mechanical Engineering, Faculty of Engineering, Kasetsart University, Bangkok 10900, Thailand.

*Corresponding author, E-mail: ovrsk@ku.ac.th

Received 6 Aug 2002

Accepted 24 Jan 2003

ABSTRACT The new compressible low-Reynolds-number q-ζ turbulence model is developed via the pressure dilatation model in order to account for the compressibility effects. The effects of the turbulent Reynolds number, the turbulence Mach number and the ratio of the production to the dissipation rate of square root of the turbulence kinetic energy are incorporated in the model for the pressure-dilatation correlation. The efficiency of the proposed model is evaluated using the compressible turbulent boundary layer flow on a flat plate at subsonic and supersonic speeds as a test case. It is found that the predicted results from the proposed model are in good agreement with the universally accepted data especially in the outer region of the boundary layer.

KEYWORDS: turbulence model, pressure dilatation, compressibility effects.

INTRODUCTION

The effect of compressibility to turbulent flows is found to be important for the flows through gas turbine, propulsion and supersonic airplane where the density changes rapidly and strongly. There are several terms directly reflect the effect of compressibility on the turbulence structure. Among these are the dilatation dissipation, the pressure dilatation and the enthalpy production. However, the present work is focused on the pressure dilatation term. The pressure dilatation is investigated to account for the extra source term that appears explicitly in the turbulence transport equation for compressible turbulent flows, due to the non-divergent fluctuating velocity field. The pressure dilatation refers to the work done due to simultaneous fluctuations in the volume of the fluid cell corresponding to the fluctuations in pressure and can be either positive or negative. The negative value represents a dissipation effect on the kinetic energy of the fluctuations and the positive value represents a production effect. The correlation between the pressure and the dilatation was found to play an important role in the exchange of energy,[1] which is also a specific phenomenon for compressible flows and can change the amount of turbulence kinetic energy rapidly.

The effect of pressure dilatation on the turbulence structure is a difficult issue in turbulence modeling. Modeling issues in both the production and dissipation of turbulence kinetic energy need to be addressed to account for Mach number effects. The modifications of this model were proposed by Zeman,[1] Sarkar,[2] El Baz and Launder,[3] Krishnamurty and Shyy,[4] and Lejeune and Kourta[5] to simulate the effect of this dilatational term. Fujiwara and Arakawa[6] have attempted to correlate the pressure fluctuation and the dilatation terms based on the direct numerical simulation (DNS) data of compressible isotropic and homogeneous sheared turbulence. They have found that the correlation between these two terms can be devised to reflect the effects of turbulence Mach number and the ratio of the production to dissipation rate of turbulence kinetic energy. Different expressions of the pressure dilatation model proposed by different researchers have been studied and it is found that the pressure dilatation model proposed by Fujiwara and Arakawa[6] gives the most accurate results for predicting the characteristics of compressible turbulent flow. Furthermore, the model is easily applied to wider applications and simple to solve. Therefore, the model of Fujiwara and Arakawa[6] is modified in this work for using with the compressible low-Reynolds-number q-ζ turbulence model.

The study of compressible turbulent flow is governed by the conservation of mass, momentum, energy and state equations. The turbulent effect is taken into account by the compressible low-Reynolds-number q-ζ turbulence model proposed by Gibson and Dafa'Alla[7] to improve the prediction of the flow characteristics near the wall, where the two dependent variables are $q\ (=\sqrt{k}\,)$ and $\zeta\ (=\varepsilon/2q)$. The square root of turbulence kinetic energy (q) is preferred to the turbulence kinetic energy (k) because in the region very close to the wall, q varies linearly with distance y. The destruction rate of the square root of turbulence kinetic energy (ζ) is better behaved than the dissipation of turbulence kinetic energy (ε). Furthermore, both q and ζ are zero at the wall and numerical problems are

alleviated because there is no need to calculate terms like $D = 2\nu\left(\partial\sqrt{k}/\partial y\right)^2$, which are needed to provide a derived boundary condition for ε in the k-ε model.

The q-ζ model was validated using the DNS data of channel flow and boundary layers,[7] and it was then applied to the calculation of the flow over 2D backward facing steps by Gibson and Harper.[8] The results showed that the q-ζ model compared well with the k-ε model in separated flows behind the steps even with the use of coarser calculation mesh. In a further development, Dafa'Alla, *et al*[9-10] applied the model to boundary layers with periodic variation of free-stream velocity and time-mean adverse pressure gradient, and Gibson and Harper[11] calculated the heat transfer from an impinging jet. The predictions compared well with the corresponding experimental data and with the k-ε model, and the q-ζ model was the more economical with coarser grids and less computing time required for convergence compared with the other methods.

The present work aims to develop and evaluate the efficiency of the proposed compressible turbulence model for the flow predictions in steady compressible turbulent boundary layer past a flat plate by applying the low-Reynolds-number q-ζ turbulence model together with the pressure dilatation model of Fujiwara and Arakawa.[6]

Governing Equations

Compressible flow is governed by the continuity, Navier-Stokes, energy and state equations. For turbulent compressible flow, these governing equations are essentially time-averaged using the density-weighting technique called Favre averaging and the resulting solution represents the mean quantities. This technique gives rise to the extra-unknown terms that cause a closure problem. This problem can be solved using an appropriate turbulence model. For steady two-dimensional mean flow, the governing equations with the turbulence model can be expressed in terms of tensor notation as follows:

Continuity Equation

$$\frac{\partial \bar{\rho}\tilde{u}_i}{\partial x_i} = 0 \tag{1}$$

Navier-Stokes Equation

$$\frac{\partial}{\partial x_j}(\bar{\rho}\tilde{u}_i\tilde{u}_j) = \frac{\partial}{\partial x_j}(\bar{t}_{ij} + \tau_{ij}) - \frac{\partial \bar{p}}{\partial x_i} \tag{2}$$

where

$$\bar{t}_{ij} = \mu\left[\left(\frac{\partial \tilde{u}_i}{\partial x_j} + \frac{\partial \tilde{u}_j}{\partial x_i}\right) - \frac{2}{3}\delta_{ij}\frac{\partial \tilde{u}_k}{\partial x_k}\right] \tag{3}$$

and τ_{ij} is from Boussinesq approximation[12]

$$\tau_{ij} = \mu_t\left[\left(\frac{\partial \tilde{u}_i}{\partial x_j} + \frac{\partial \tilde{u}_j}{\partial x_i}\right) - \frac{2}{3}\delta_{ij}\frac{\partial \tilde{u}_k}{\partial x_k}\right] - \frac{2}{3}\delta_{ij}\bar{\rho}q^2 \tag{4}$$

Energy Equation

$$\frac{\partial}{\partial x_j}(\bar{\rho}\tilde{u}_j\tilde{e}_T) = \frac{\partial}{\partial x_j}\left[\left(\frac{k_T}{C_V} + \mu_t\right)\frac{\partial \tilde{e}_T}{\partial x_j}\right] + \frac{\partial}{\partial x_j}\left[\tilde{u}_i\left(\bar{t}_{ij} + \tau_{ij}\right)\right] - \frac{\partial}{\partial x_j}\left(\tilde{u}_j\bar{p}\right) + \frac{\partial}{\partial x_j}\left[\left(\mu + \mu_t\right)\frac{\partial q^2}{\partial x_j}\right] - \frac{\partial}{\partial x_j}\left[\left(\frac{k_T}{C_V} + \mu_t\right)\frac{\partial}{\partial x_j}(K + q^2)\right] \tag{5}$$

where $\tilde{e}_T$ is defined as

$$\tilde{e}_T = \tilde{e} + K + q^2 \tag{6}$$

and

$$\tilde{e} = C_v\tilde{T},\ K = 0.5\left(\tilde{u}^2 + \tilde{v}^2\right) \tag{7}$$

Compressible Low-Reynolds-Number q-ζ Turbulence Model

The eddy viscosity (μ_t) can be defined as

$$\mu_t = \bar{\rho} C_\mu f_\mu \frac{q^3}{2\zeta} \tag{8}$$

The Favre-averaged equations for q and ζ are given by

$$\frac{\partial}{\partial x_j}(\bar{\rho}\tilde{u}_j q) = \frac{\partial}{\partial x_j}\left[(\mu + \mu_t)\frac{\partial q}{\partial x_j}\right] + \frac{\tau_{ij}}{2q}\frac{\partial \tilde{u}_i}{\partial x_j} - \bar{\rho}\zeta + \overline{p'\frac{\partial u_i''}{\partial x_j}} \tag{9}$$

$$\frac{\partial}{\partial x_j}(\bar{\rho}\tilde{u}_j \zeta) = \frac{\partial}{\partial x_j}\left[\left(\mu + \frac{\mu_t}{\sigma_\zeta}\right)\frac{\partial \zeta}{\partial x_j}\right] + C_{\zeta 1} f_{\zeta 1}\frac{\zeta}{q^2}\tau_{ij}\left(\frac{\partial \tilde{u}_i}{\partial x_j} + \frac{1}{3}\frac{\partial \tilde{u}_k}{\partial x_k}\delta_{ij}\right)$$
$$- \bar{\rho} C_{\zeta 2} f_{\zeta 2}\frac{\zeta^2}{q} - \frac{4}{3}\bar{\rho}\zeta\frac{\partial \tilde{u}_k}{\partial x_k} + \bar{\rho}\psi \tag{10}$$

where $\sigma_\zeta, C_{\zeta 1} f_{\zeta 1}, C_{\zeta 2} f_{\zeta 2}$ and ψ are equivalent to $\sigma_\varepsilon, 2C_{\varepsilon 1} f_{\varepsilon 1} - 1, 2C_{\varepsilon 2} f_{\varepsilon 2} - 1$ and $\frac{E}{2q}$, respectively, in the low-Reynolds-number k-ε models. The constants $(\sigma_k, \sigma_\varepsilon, C_\mu, C_{\varepsilon 1}, C_{\varepsilon 2})$, damping functions $(f_{\varepsilon 1}, f_{\varepsilon 2})$ and E are adopted from the low-Reynolds-number k- model of Launder and Sharma[13] in Table 1.

The extra term E is

$$E = 2\nu\nu_t\left(\frac{\partial^2 \tilde{u}_i}{\partial x_j \partial x_k}\right)^2 \tag{11}$$

The damping function (f_μ) proposed by Gibson and Dafa'Alla[7] is written as

$$f_\mu = \exp\left(\frac{-6}{\left(1 + \frac{Re_t}{50}\right)^2}\left(1 + 3\exp\left(\frac{-Re_t}{10}\right)\right)\right) \tag{12}$$

Table 1. Constants and damping functions of Launder-Sharma k-ε turbulence model[13]

Variables	Model constants and damping functions
σ_k	1.0
$\sigma\varepsilon$	1.3
$C\mu$	0.09
$C\varepsilon_1$	1.44
$C\varepsilon_2$	1.92
$f\varepsilon_1$	1.0
$f\varepsilon_2$	1-0.3 exp (-Re_t^2)

where the turbulent Reynolds number is defined as

$$Re_t = \frac{q^3}{2\nu\zeta} \tag{13}$$

Equation of State

$$\bar{p} = (\gamma - 1)\bar{\rho}\left(\tilde{e}_T - K - q^2\right) \tag{14}$$

Sutherland's Law

$$\mu = \mu_\infty\left(\frac{\tilde{T}}{T_\infty}\right)^{\frac{3}{2}}\frac{T_\infty + 110}{\tilde{T} + 110} \tag{15}$$

Prandtl Number

$$Pr = \frac{\mu C_p}{k_T} \tag{16}$$

Pressure Dilatation Model

The pressure dilatation term is resulted from using Favre-averaging on the square root of turbulence kinetic energy equation that represents in the last term of Equation (9). The model for pressure-dilatation correlation incorporates the effects of the turbulent Reynolds number (Re_t), turbulence Mach number (M_t)

and ratio of the production to the dissipation rate of square root of the turbulence kinetic energy (P_q/ζ).

The model can be expressed as (Fujiwara and Arakawa[6])

$$\overline{p' \frac{\partial u_i''}{\partial x_j}} = \overline{p'd'} = f_{\Pi d}\sqrt{\overline{p'^2}}\sqrt{\overline{d'^2}} \tag{17}$$

where and are the pressure variance and the dilatation variance, respectively.

The pressure variance is related to the velocity fluctuation and the function of the ratio of production to dissipation rate of the square root of turbulence kinetic energy as:

$$\sqrt{\overline{p'^2}} = C_p \bar{\rho} q^2 \tag{18}$$

where $C_p = C_{p1} + C_{p2}\frac{P_q}{\zeta}$

The dilatation variance appears in the dilatation dissipation term (ζ) and is related to turbulence Mach number as:

$$\overline{d'^2} \propto C_p^2 M_t^2 \frac{\zeta}{\nu} \tag{19}$$

(19)

where $M_t = \frac{q}{a}$ and is the speed of sound.

The correlation coefficient ($f\Pi_d$) is included in the magnitude part and the sign part. The magnitude part depends on the turbulent Reynolds number and the sign part depends on the effect of P_q/ζ.

$$f_{\Pi d} = -C_{\Pi d}\tanh\left(\frac{C_{re}}{\sqrt{Re_t}}\right)\left[\tanh\left(\frac{P_q}{\zeta C_{pe}}\right) - 0.5\right] \tag{20}$$

Finally, a model for pressure dilatation is

$$\overline{p'd'} = -C_{\Pi d}\sqrt{Re_t}\tanh\left(\frac{C_{re}}{\sqrt{Re_t}}\right)\left[\tanh\left(\frac{P_q}{\zeta C_{pe}}\right) - 0.5\right]\left(C_{p1} + C_{p2}\frac{P_q}{\zeta}\right)^2 M_t \bar{\rho}\zeta \tag{21}$$

where $P_q = -\bar{\rho}\overline{u_i'' u_j''}\frac{\partial \bar{u}_i}{\partial x_i}$, $M_t = \frac{q}{\sqrt{\gamma R\tilde{T}}}$ and the constants are as in Table 2. The expression in the above equation shows that the pressure dilatation model is a function of the turbulent Reynolds number, the turbulence Mach number and the ratio of the production to the dissipation rate of square root of the turbulence kinetic energy.

Numerical Solution Procedure

The finite volume method is used to numerically solve the governing equations, which can be written in a general form as follows:

$$\frac{\partial}{\partial x_i}\left(\rho \bar{u}_i \phi\right) = \frac{\partial}{\partial x_i}\left(\Gamma \frac{\partial \phi}{\partial x_i}\right) + S^{\phi} \tag{22}$$

Table 2. Constants for Fujiwara and Arakawa pressure dilatation model.[6]

Variables	Model constants
C_{pe}	1.0
C_{p1}	0.4
C_{p2}	0.3
$C_{\Pi d}$	0.1
C_{re}	30.0

where is the general dependent variable, is the effective diffusion coefficient, and is the source/sink term of . To simulate the internal flow with variable cross-sectional area and the external flow past an object of complex shape, the general form of the governing equations is essentially transformed from the physical domain into the computational domain using the following equation:

$$\frac{\partial}{\partial\xi}(\rho U\phi)+\frac{\partial}{\partial\eta}(\rho V\phi)=\frac{\partial}{\partial\xi}\left[\frac{\Gamma}{J}\left(\alpha\frac{\partial\phi}{\partial\xi}-\beta\frac{\partial\phi}{\partial\eta}\right)\right]+\frac{\partial}{\partial\eta}\left[\frac{\Gamma}{J}\left(\gamma\frac{\partial\phi}{\partial\eta}-\beta\frac{\partial\phi}{\partial\xi}\right)\right]+JS^{\phi} \tag{23}$$

where

$$U=\bar{u}\frac{\partial y}{\partial\eta}-\bar{v}\frac{\partial x}{\partial\eta},\quad V=\bar{v}\frac{\partial x}{\partial\xi}-\bar{u}\frac{\partial y}{\partial\xi},$$

$$\alpha=\left(\frac{\partial x}{\partial\eta}\right)^2+\left(\frac{\partial y}{\partial\eta}\right)^2,\quad \beta=\frac{\partial x}{\partial\xi}\frac{\partial x}{\partial\eta}+\frac{\partial y}{\partial\xi}\frac{\partial y}{\partial\eta},\quad \gamma=\left(\frac{\partial x}{\partial\xi}\right)^2+\left(\frac{\partial y}{\partial\xi}\right)^2,$$

$$J=\frac{\partial x}{\partial\xi}\frac{\partial y}{\partial\eta}-\frac{\partial y}{\partial\xi}\frac{\partial x}{\partial\eta}.$$

Using the finite volume method, the computational domain is divided into a number of control volumes. The transformed equations can be integrated as follows:

$$[(\rho U\Delta\eta)\phi]_w^e+[(\rho V\Delta\xi)\phi]_s^n=\left[\frac{\Gamma\Delta\eta}{J}\left(\alpha\frac{\partial\phi}{\partial\xi}-\beta\frac{\partial\phi}{\partial\eta}\right)\right]_w^e+\left[\frac{\Gamma\Delta\xi}{J}\left(\gamma\frac{\partial\phi}{\partial\eta}-\beta\frac{\partial\phi}{\partial\xi}\right)\right]_s^n+(J\Delta\xi\Delta\eta)\bar{S}_P^{\phi} \tag{24}$$

where $\bar{S}_P^{\phi}$ is the mean value of S^{ϕ} at the center P of each control volume, and (e, w, n, s) are the east, west, north and south faces of each control volume. The convection terms are approximated by the first-order upwind differencing scheme and the diffusion terms are estimated by the second-order central differencing scheme. Therefore, the standard form of the finite volume equation can be obtained as

$$A_P^{\phi}\phi_P=A_E^{\phi}\phi_E+A_W^{\phi}\phi_W+A_N^{\phi}\phi_N+A_S^{\phi}\phi_S+b^{\phi} \tag{25}$$

where

$$A_E^{\phi}=\left(\frac{\Gamma}{J}\alpha\frac{\Delta\eta}{\Delta\xi}\right)_e+\max[0,-(\rho U\Delta\eta)_e],\quad A_W^{\phi}=\left(\frac{\Gamma}{J}\alpha\frac{\Delta\eta}{\Delta\xi}\right)_w+\max[0,(\rho U\Delta\eta)_w],$$

$$A_N^{\phi}=\left(\frac{\Gamma}{J}\gamma\frac{\Delta\xi}{\Delta\eta}\right)_n+\max[0,-(\rho V\Delta\xi)_n],\quad A_S^{\phi}=\left(\frac{\Gamma}{J}\gamma\frac{\Delta\xi}{\Delta\eta}\right)_s+\max[0,(\rho V\Delta\xi)_s],$$

$$A_P^{\phi}=A_E^{\phi}+A_W^{\phi}+A_N^{\phi}+A_S^{\phi},$$

$$b^{\phi}=(J\Delta\xi\Delta\eta)\bar{S}_P^{\phi}-\left[\frac{\Gamma\Delta\eta}{J}\left(\beta\frac{\partial\phi}{\partial\eta}\right)\right]_w^e-\left[\frac{\Gamma\Delta\xi}{J}\left(\beta\frac{\partial\phi}{\partial\xi}\right)\right]_s^n.$$

The standard SIMPLE algorithm[14] is employed here to satisfy the conservation law of mass. The continuity equation is not solved directly with other governing equations. The p'-equation is solved instead to obtain the pressure correction p' and its value is used to correct the values of pressure and velocities to satisfy the conservation law of mass. The p'-equation can be written in a standard form as follows:

$$A_P^p p'_P=A_E^p p'_E+A_W^p p'_W+A_N^p p'_N+A_S^p p'_S+m_P \tag{26}$$

where

$$A_E^p = \left(\rho B \frac{\Delta\eta}{\Delta\xi}\right)_e, \; A_W^p = \left(\rho B \frac{\Delta\eta}{\Delta\xi}\right)_w, \; A_N^p = \left(\rho C \frac{\Delta\xi}{\Delta\eta}\right)_n, \; A_S^p = \left(\rho C \frac{\Delta\xi}{\Delta\eta}\right)_s,$$

$$A_P^p = A_E^p + A_W^p + A_N^p + A_S^p, \; \dot{m}_P = \left(\rho U^* \Delta\eta\right)_w - \left(\rho U^* \Delta\eta\right)_e + \left(\rho V^* \Delta\xi\right)_s - \left(\rho V^* \Delta\xi\right)_n.$$

U^* and V^* are calculated from the resulting velocities of the Navier-Stokes equations, whereas

$$B = B^u \frac{\partial y}{\partial \eta} - B^v \frac{\partial x}{\partial \eta}, \quad C = C^v \frac{\partial x}{\partial \xi} - C^u \frac{\partial y}{\partial \xi} \tag{27}$$

where

$$B^u = -\frac{\Delta\xi\Delta\eta}{A_P^u}\frac{\partial y}{\partial \eta}, \; B^v = \frac{\Delta\xi\Delta\eta}{A_P^v}\frac{\partial x}{\partial \eta}, \; C^u = \frac{\Delta\xi\Delta\eta}{A_P^u}\frac{\partial y}{\partial \xi}, \; C^v = -\frac{\Delta\xi\Delta\eta}{A_P^v}\frac{\partial x}{\partial \xi}.$$

In general, the standard SIMPLE algorithm is implemented on the staggered grid system to prevent the decoupling between the velocity and the pressure. However, the staggered grid system is technically rather complicated for programming and requires a large amount of computer storage. This drawback becomes obvious when the computer program is developed further for real-world applications. The collocated grid system is employed in this work so that all the variables are stored at the center of each control volume. The problem of velocity-pressure decoupling is solved by the Rhie and Chow interpolation[15] where (U_e^*, U_w^*, V_n^*, V_s^*) are calculated from the appropriate pressure gradient.

Results and Discussion

The test case for compressible turbulent flow over a flat plate is chosen in this work to evaluate the efficiency of the compressible q-ζ turbulence model together with the pressure dilatation model in predicting the compressible turbulent boundary layer. According to grid independent study, a grid of 151×151 nodes in cross-stream and streamwise directions is used respectively. The schematic representation of flat plate can be seen in Fig 1.

The performance of the model is evaluated via the closeness of the compared parameters to the universally accepted data in comparison with the conventional compressible q-ζ turbulence model. The compared parameters and the universally accepted data are shown in Table 3. The comparison will be presented for parameters at Mach number 0.82 and 1.50.

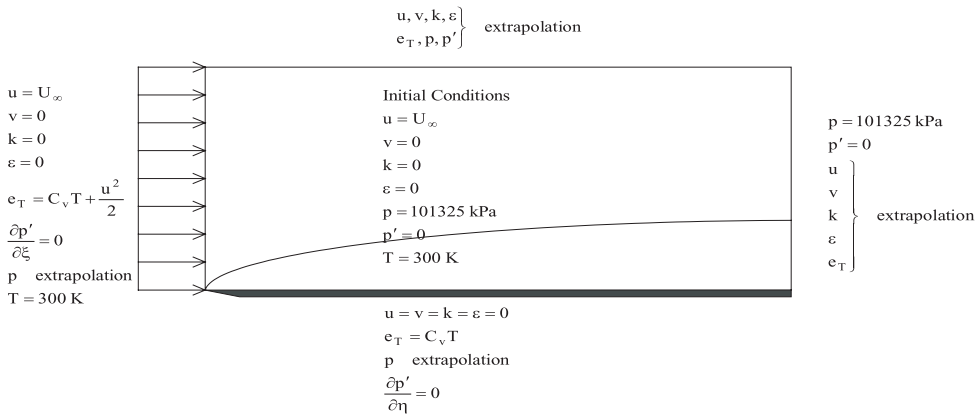

Fig 1. Schematic representation of computational domain.

Table 3. The comparisons between the compared parameters and the universally accepted data.

Compared parameters	Universally accepted data
Velocity distribution for inner region	Law of the wall
Velocity distribution for outer region	Maise and McDonald[16]
Velocity distribution for outer region	Fernholz and Finley[17]
Skin friction coefficient distribution	Nash and MacDonald[18]

Inner Region

The law of the wall represents the velocity profile outside the laminar sublayer and in the logarithmic region ($3.6 < y^+ < 8.0$), which is expressed as

$$\frac{u^*}{u_\tau} = \frac{1}{\kappa}\ln y^+ + c \qquad (28)$$

where the values of constants κ and were taken as 0.4 and 5.1, respectively.

The transformed velocity (u^*) that is derived from the Van Driest transformation[19] and the concept of temperature recovery factor (r) is given by

$$u^* = \frac{\tilde{u}_\delta}{b}\sin^{-1}\left[\frac{2b^2\frac{\tilde{u}}{\tilde{u}_\delta} - a}{\sqrt{a^2+4b^2}}\right] \qquad (29)$$

where

$$a = \frac{\tilde{T}_\delta}{\tilde{T}_w}\left[1 + r\frac{\gamma-1}{2}M_\delta^2\right] - 1, \text{ and } b^2 = r\frac{\gamma-1}{2}M_\delta^2\frac{\tilde{T}_\delta}{\tilde{T}_w}.$$

Fig 2 shows the velocity distribution of the turbulent boundary layer on a flat plate at Mach number 0.82 where the computed results are compared with the law of the wall. It is found that in the logarithmic region, the velocity distribution of the model with pressure dilatation shifts from the law of the wall. This is because the pressure dilatation model takes into account the damping effect of pressure variation near the wall that results in the increase of the velocity distribution in the boundary layer.

The velocity distribution at Mach number 1.50 is shown in Fig 6. The deviation of velocity distribution of model with pressure dilatation is higher than the case of Mach number 0.82 because the effect of Mach number on the velocity distribution is brought to bear through the increase of temperature in the direction of the wall.

Outer Region

Maise and McDonald[16] correlation extends the validity of the Van Driest transformation to the outer region of boundary layer by introducing u^* into the velocity defect law with a finite wake component. In the experiment of Motallebi[20], it also predicts the correct trend of the data. Maise and McDonald correlation is defined as

$$\frac{u_\delta^* - u^*}{u_\tau} = -2.5\ln\frac{y}{\delta} + 1.25\left[1 + \cos\left(\pi\frac{y}{\delta}\right)\right] \qquad (30)$$

where $u\tau = \sqrt{\tau_w / \bar{\rho}_w}$.

Fig 3 and 7 show the velocity distribution of the turbulent boundary layer on a flat plate at Mach number 0.82 and 1.50 respectively, where the computed results are compared with Maise and McDonald correlation. It is found that the computed results of the developed model are in good agreement with this correlation at outer region ($0.2 \le \frac{y}{\delta} \le 1.0$). This is a consequence of the pressure dilatation model in the compressible turbulence model.

Fernholz and Finley[17] have achieved a better correlation for the outer region of boundary layer with a semi-empirical semiempirical relationship. In this expression, the constant terms are obtained from a correlation of experimental data. Fernholz and Finley correlation compares very well with the experimental data of Motallebi.[20] Fernholz and Finley correlation is defined as

$$\frac{u_\delta^* - u^*}{u_\tau} = -4.7\ln\frac{y}{\Delta^*} - 6.74 \qquad (31)$$

where $\Delta^* = \delta\int_0^1\left(\frac{u_\delta^* - u^*}{u_\tau}\right)d\left(\frac{y}{\delta}\right)$

Fig 4 and 8 show the comparison of velocity distribution with Fernholz and Finley correlation at Mach number 0.82 and 1.50, respectively. It is found that the results of the model with pressure dilatation are closer than the model without pressure dilatation.

Skin Friction Coefficient

The skin friction coefficient values are deduced using the expression proposed by Nash and MacDonald[18] correlation, which depends on the integral quantities of boundary layer. Nash and MacDonald correlation is expressed as

$$\frac{C_f}{2} = \left\{F_C^{1/2}\left[2.4711\ln(F_R\,Re_\theta) + 4.75\right] + 1.5G + \frac{1724}{G^2+200} - 16.87\right\}^{-2} \qquad (32)$$

in which

$$F_C^{1/2} = 1 + 0.066M_\delta^2 - 0.008M_\delta^3\mu \qquad (33)$$

$$F_R = 1 - 0.134M_\delta^2 + 0.027M_\delta^3 \qquad (34)$$

$$G = 6.1\sqrt{\beta + 1.81} - 1.7 \qquad (35)$$

with $\beta = 0$ in the present work.

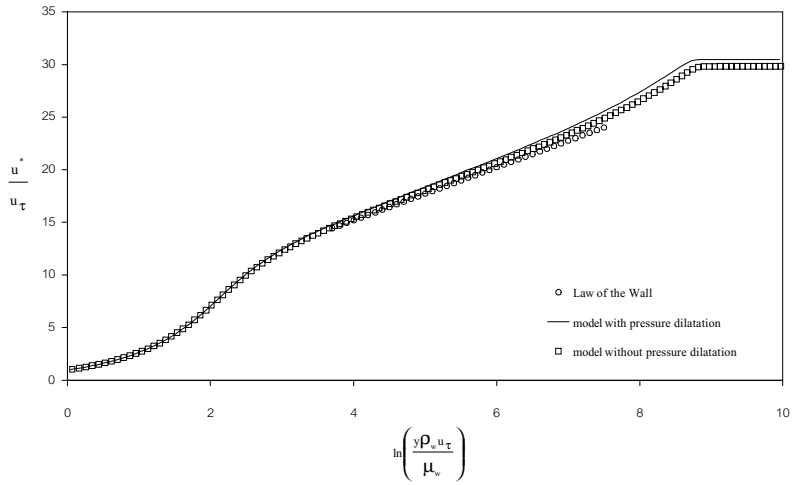

Fig 2. Velocity distribution of the turbulent boundary layer on a flat plate at Mach number 0.82 for inner region.

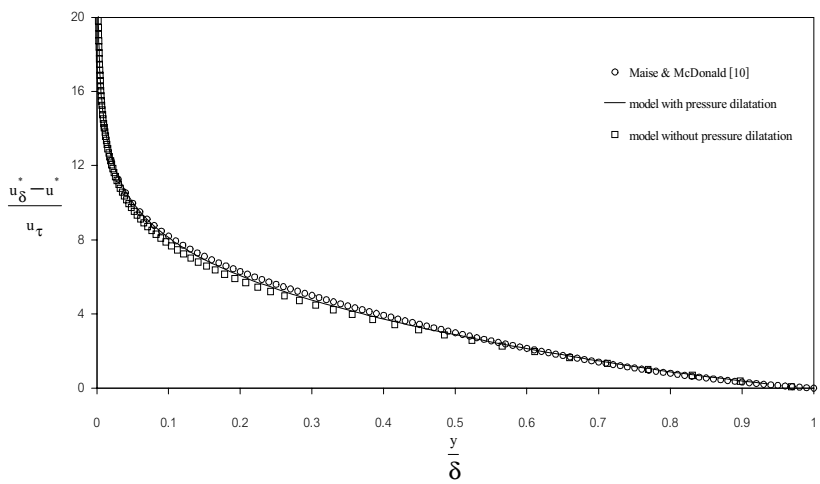

Fig 3. Velocity distribution of the turbulent boundary layer on a flat plate at Mach number 0.82 for outer region (compared with the Maise and NcDonald correlation).

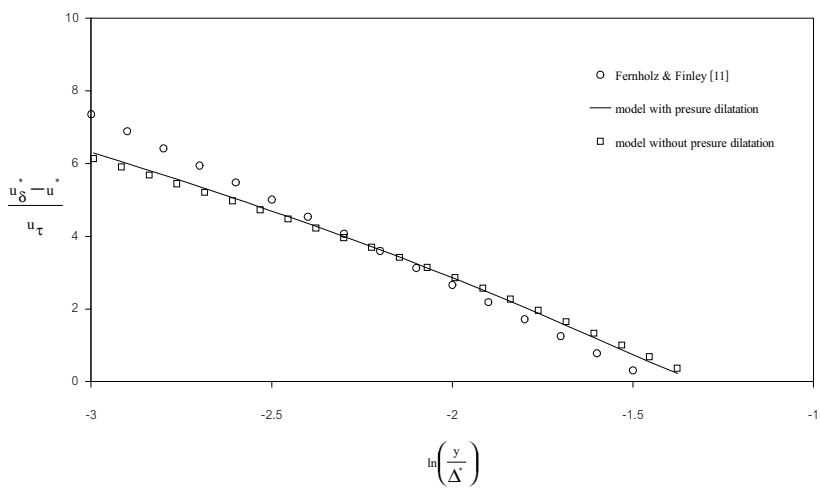

Fig 4. Velocity distribution of the turbulent boundary layer on a flat plate at Mach number 0.82 for outer region (compared with the Fernholz and Finley correlation).

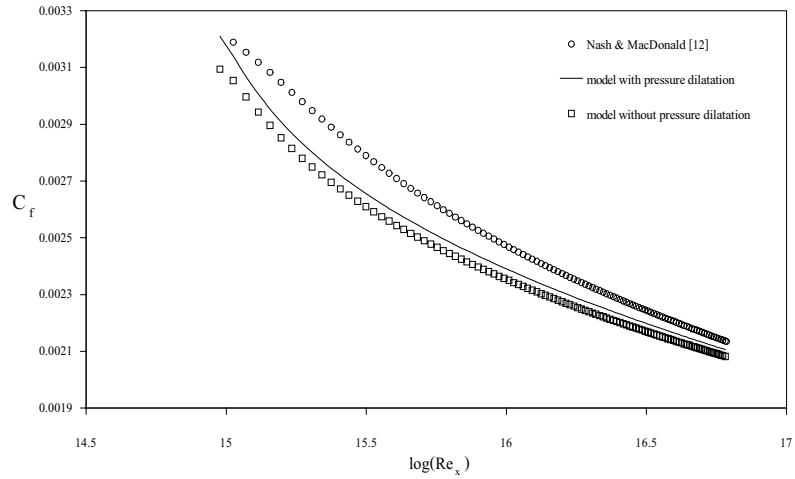

Fig 5. Skin friction coefficient distribution of the turbulent boundary layer on a flat plate at Mach number 0.82.

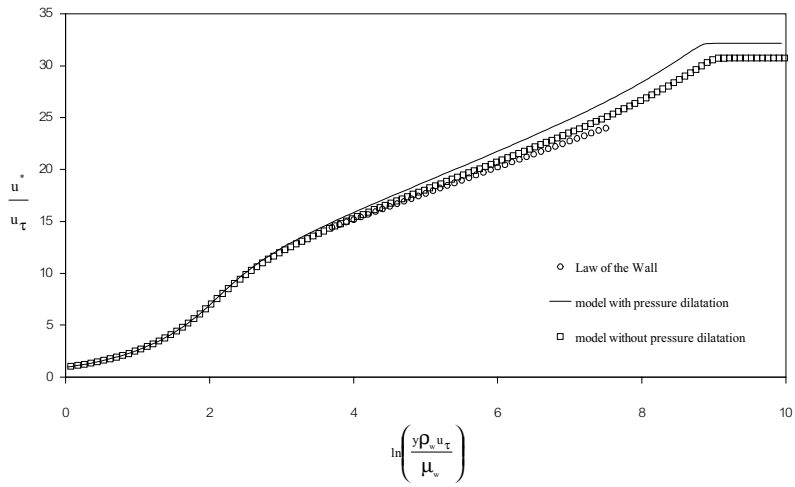

Fig 6. Velocity distribution of the turbulent boundary layer on a flat plate at Mach number 1.50 for inner region.

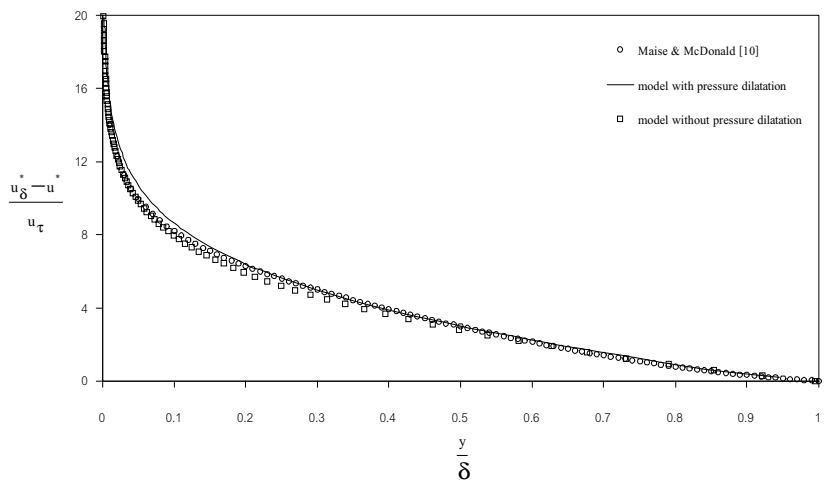

Fig 7. Velocity distribution of the turbulent boundary layer on a flat plate at Mach number 1.50 for outer region (compared with the Maise and McDonald correlation).

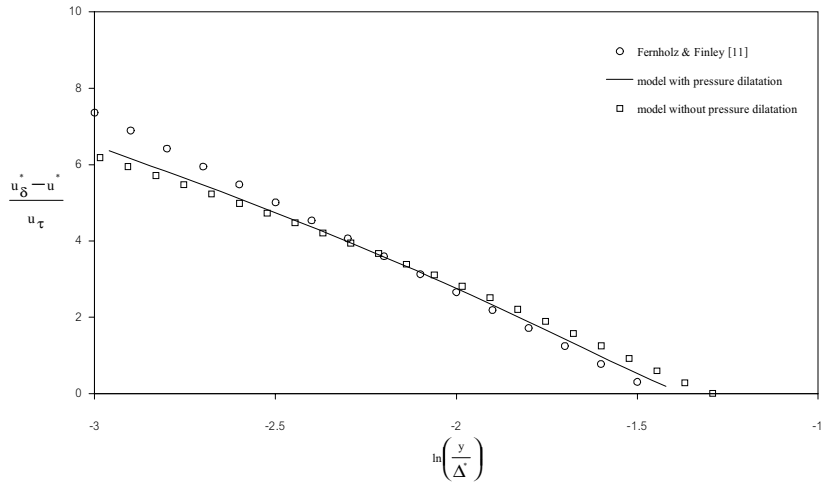

Fig 8. Velocity distribution of the turbulent boundary layer on a flat plate at Mach number 1.50 for outer region (compared with the Fernholz and Finley correlation).

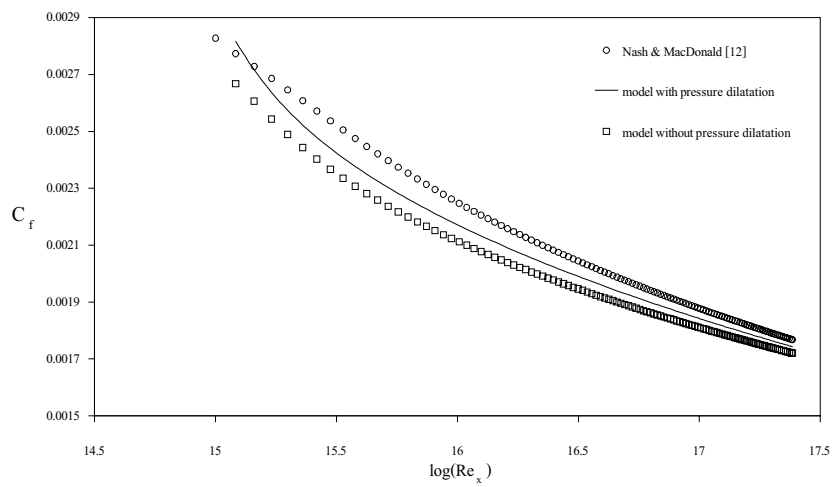

Fig 9. Skin friction coefficient distribution of the turbulent boundary layer on a flat plate at Mach number 1.50.

Fig 5 and 9 show the comparison of the skin friction coefficient distribution with Nash and MacDonald correlation at Mach number 0.82 and 1.50, respectively. It is found that the computed results of the model with pressure dilatation are in reasonable agreement with Nash and MacDonald. The effect of pressure dilatation model causes the skin friction coefficient to increase compared to the model without pressure dilatation for both Mach numbers.

The deviation in the results is due to the coefficient of skin friction and does not include the effect of the laminar initial length. In reality, the boundary layer is laminar to begin with, undergoes transition, and changes to turbulence further downstream. The existence of the laminar section causes the skin friction coefficient to decrease. Additionally, the increases in the Mach number and the viscosity result in the decrease in the skin friction coefficient.

Conclusions

The compressibility effects are incorporated in the low-Reynolds-number q-ζ turbulence model via the modification of the pressure dilatation model of Fujiwara and Arakawa. The effects of the turbulent Reynolds number, the turbulence Mach number and the ratio of the production to the dissipation rate of the square root of turbulence kinetic energy are incorporated in the model for the pressure-dilatation correlation. The computed results using the developed model are compared with the universally accepted data for two-dimensional compressible equilibrium turbulent boundary layers. It is found that the predicted solutions using the developed model are in good agreement with the experimental data especially in the outer region of the boundary layer.

ACKNOWLEDGEMENTS

This research is partially supported by the Thailand Research Fund for (to Professor Pramote Dechaumphai), the Kasetsart University Research and Development Institute and the Thesis and Dissertation Support Fund, Graduate School, Kasetsart University. Special thanks are due to Professor Pramote Dechaumphai and Assistant Professor Ekachai Juntasaro.

Appendix A. Nomenclature

a = parameter in Van Driest transformation; speed of sound,
b = parameter in Van Driest transformation
C_f = skin friction coefficient
C_p = specific heat at constant pressure
C_V = specific heat at constant volume
$C\mu$ = model constant for eddy viscosity
$C\varepsilon_1$, $C\varepsilon_2$, $C\zeta_1$, $C\zeta_2$ = model constants for turbulence model
C_{p1}, C_{p2}, C_{pe}, C_{re}, $C\Pi_d$ = model constants for pressure dilatation model
c = intercept for Coles law of the wall
D = extra term for turbulence kinetic energy equation
d = dilatation part
E = extra term for dissipation rate of turbulence kinetic energy equation
e = internal energy
e_T = specific total energy
F_C, F_R = parameters in Nash and MacDonald skin friction correlation
$f\mu$ = damping function for eddy viscosity
$f\varepsilon_1$, $f\varepsilon_2$, $f\zeta_1$, $f\zeta_2$ = model functions for turbulence model
$f\Pi_d$ = correlation coefficient between pressure and dilatation fluctuation
G = parameter in Nash and MacDonald skin friction correlation
K = kinetic energy
k = turbulence kinetic energy
k_T = thermal conductivity
M = Mach number
M_t = turbulence Mach number
p = pressure
Pr = Prandtl's number
P_q = production of the square root of turbulence kinetic energy
q = square root of turbulence kinetic energy
R = gas constant, 287 J/kg.-K for air
Re_t = turbulent Reynolds number
$Re\theta$ = momentum thickness Reynolds number
r = temperature recovery factor, 0.89
T = temperature
t = laminar shear stress
u = velocity
$u\tau$ = friction velocity
y = wall-normal coordinate
y^+ = dimensionless distance from wall, $y\rho_w u\tau/\mu_w$ for inner region and y/δ for outer region
δ = boundary-layer thickness
δ_{ij} = Kronecker delta, for and for
Δ^* = integral length scale
ε = rate of dissipation of turbulence kinetic energy
γ = ratio of specific heat, 1.4 for air
κ = slope for Coles law of the wall
μ = fluid viscosity
μ_t = eddy viscosity
ν = kinematic viscosity
ρ = density
σ_q, $\sigma\zeta$ = model constants for turbulent diffusion
τ = turbulent shear stress
ζ = rate of dissipation of the square root of turbulence kinetic energy

Subscripts

w = evaluated based on wall parameters
δ = boundary-layer edge
∞ = freestream

Superscripts

′ = fluctuation part of Reynolds decomposition
″ = fluctuation part of Favre decomposition
– = Reynolds average
~ = Favre average
* = tranformed condition

REFERENCES

1. Zeman O (1993) New model for super/hypersonic turbulent boundary layers. *AIAA Paper 93-0897*.
2. Sarkar S (1992) The pressure dilatation correlation in compressible flows. *Physics of Fluid* **4**, 2674-82.
3. El Baz AM and Launder BE (1996) Second-moment modeling of compressible mixing layer. In: *Engineering Turbulence Modeling and Experiments*, pp 63-72. Elsevier Science, New York.
4. Krishnamurty VS and Shyy W (1997) Compressibility effects in modeling complex turbulent flows. *Prog. Aerospace Sci.* **33**, 587-645.
5. Lejeune C and Kourta A (1997) Modeling of extra-compressibility terms in high speed turbulent flows. *International Conference of Turbulent Shear Flow*.
6. Fujiwara H and Arakawa C (1996) Modeling of compressible turbulent flows with emphasis on pressure-dilatation correlation. In: *Engineering Turbulence Modeling and Experiments3* (Edited by Rodi W and Bergeles G), pp 151-60.
7. Gibson MM and Dafa'Alla AA (1994) Two-equation model for turbulent wall flow. *AIAA Journal* **33**, 1514-18.
8. Gibson MM and Harper RD (1995) Calculations of separated flows with the low-Reynolds-number q-ζ turbulence model. *10th Symposium on Turbulent Shear Flows*, Pennsylvania State University, USA.
9. Dafa'Alla AA, Juntasaro E and Gibson MM (1996) Calculation of oscillating boundary layers with the q-ζ turbulence model. In: *Engineering Turbulence Modelling and Experiments 3* (Edited by Rodi W and Bergeles G), pp 141-50. Elsevier Science.

10. Dafa'Alla AA, Juntasaro E and Gibson MM (1997) Computations of periodic turbulent boundary layers with moderate adverse pressure gradient. *International Journal of Heat and Fluid Flow* **18**, 443-51.
11. Gibson MM and Harper RD (1997) Calculation of impinging-jet heat transfer with the low-Reynolds-number q-ζ turbulence model. *International Journal of Heat and Fluid Flow* **18**, 80-7.
12. Boussinesq J (1877) Theory de L'ecoulment tourbillant. *Memoires Presentes Par Divers Savants Sciences Mathematique at Physiques* **23**, 46-50. Academie de Sciences. 13. Launder BE and Sharma BI (1974) Application of the energy-dissipation model of turbulence to the calculation of a flow near a spinning disk. *Letters in Heat and Mass Transfer* **1**, 131-8.
14. Patankar SV and Spalding DB (1972) A calculation procedure for heat, mass and momentum transfer in three-dimensional parabolic flows. *International Journal of Heat and Mass Transfer* **15**, 1787-806.
15. Rhie CM and Chow WL (1983) Numerical study of the turbulent flow past an airfoil with trailing edge separation. *AIAA Journal* **21**, 1525-32.
16. Maise G and McDonald H (1968) Mixing length and kinematic eddy viscosity in a compressible boundary layer. *AIAA Journal* **6**, 73-80.
17. Fernholz HH and Finley PJ (1980) A critical commentary on mean flow data for two-dimensional compressible turbulent boundary layers. *AGARDograph*.
18. Nash JF and MacDonald AGJ (1966) A turbulent skin-friction law for use at subsonic and transonic speeds. *NPL Aero Rept 1206*. National Physics Lab. Teddington, England.
19. Van Driest ER (1951) Turbulent boundary layer in compressible fluids. *Journal of Aeronautical Sciences* **18**, 145-60.
20. Motallebi F (1994) Mean flow study of two-dimensional subsonic turbulent boundary layers. *AIAA Journal* **32**, 2153-61.